

## Power grand composite curves shaping for adaptive energy management of hybrid microgrids



Damian Giaouris<sup>a, d</sup>, Athanasios I. Papadopoulos<sup>a, \*</sup>, Panos Seferlis<sup>a, c</sup>,  
Spyros Voutetakis<sup>a</sup>, Simira Papadopoulou<sup>a, b</sup>

<sup>a</sup> Chemical Process and Energy Resources Institute, Centre for Research and Technology Hellas, Thessaloniki, Greece

<sup>b</sup> Department of Automation Engineering, Alexander Technological Educational Institute of Thessaloniki, Thessaloniki, Greece

<sup>c</sup> Aristotle University of Thessaloniki, Department of Mechanical Engineering, Thessaloniki, Greece

<sup>d</sup> Newcastle University, School of Electrical and Electronic Engineering, Newcastle Upon Tyne, UK

### ARTICLE INFO

#### Article history:

Received 23 November 2015

Received in revised form

28 March 2016

Accepted 16 April 2016

#### Keywords:

Energy management

Power pinch analysis

Grand composite curves

Hybrid renewable energy systems

Process integration

### ABSTRACT

This work proposes a systematic approach for the adaptive identification and implementation of efficient power management strategies (PMS) in the course of operation of hybrid renewable energy microgrids. The approach is based on the temporal evolution of the system power grand composite curve (PGCC), which is adaptively shaped on-line and within short-term time intervals to form a sequence of decisions indicating the instant and duration of activation of different subsystems. It builds on from previous work where the potential for system performance enhancement could not be exploited through pre-specified PMS identified off-line. More specifically, it involves a stored energy targeting step that exploits the PGCC to identify the desired operational profile of an accumulator during a prediction horizon in order to satisfy the system operating goals. The identified energy targets are subsequently enforced through a sequence of control actions that enable the exact matching of the PGCC hence resulting in a new PMS. The method is elaborated graphically for multiple potential operating goals and is supported by a formal mathematical model that captures system structural and temporal characteristics. It is implemented on an actual hybrid microgrid considering multiple RES-based energy generation and storage options for expected and unexpected weather conditions.

© 2016 Elsevier Ltd. All rights reserved.

### 1. Introduction

Micro grids based on renewable energy sources (RES) are receiving increased attention worldwide as they are required to support isolated and non-grid connected applications. To address the intermittent nature of largely unpredictable environmental phenomena, such systems transform RES into dependable energy flows by simultaneous utilization of different types of conversion equipment and storage media (e.g. PV panels, wind generators, chemical energy accumulators, hydrogen and so forth). The resulting infrastructures combine multiple subsystems of heterogeneous characteristics that need to operate efficiently while satisfying power demands based entirely on RES. The complex synergies and interactions that emerge among such components raise the need for efficient decision making as potential operating

alternatives unravel simultaneously with an increasing number of diverse components that become involved in the operations of the system. This decision making is generally addressed through power management strategies (PMS) [7] which represent a complex sequence of actions offering efficient utilization of resources and equipment to meet specific targets. Such actions account for decisions regarding the appropriate instant to activate/deactivate different subsystems, the duration of operation of a particular subsystem, the amount or type of energy carrier to use (e.g., electricity, hydrogen in high or low pressure, water) and so forth. They also depend on several criteria involving the availability of power from RES with respect to the demand (lack or excess), the availability of energy carriers in storage and the previous state of operation of different sub-systems [11], to name but a few. Such diverse characteristics give rise to a large number of potential PMS. Efficient operation depends on the selection of the PMS that best satisfies the demands of the targeted application in view of RES variability, while maintaining a smooth system operation and

\* Corresponding author.

E-mail address: [spapadopoulos@cperi.certh.gr](mailto:spapadopoulos@cperi.certh.gr) (A.I. Papadopoulos).

Nomenclature	
<i>BAT</i>	battery
<i>BF</i>	low pressure (buffer) storage tanks
$C_l$	capacity of accumulator <i>l</i>
<i>CMP</i>	compressor
<i>DSL</i>	diesel generator
<i>EL</i>	electrolyser
$F_{m \rightarrow n}^j(t)$	state of the flow <i>j</i> between the nodes <i>m</i> and <i>n</i>
<i>FC</i>	fuel cell
<i>FT</i>	long-term storage tank
<i>H</i>	overall time span
<i>H2HP</i>	hydrogen in high pressure
<i>H2LP</i>	hydrogen in low pressure
<i>H2O</i>	water
<i>L</i>	logical operator
<i>LD</i>	load
$Lo_i^{SOAcc^l}$	lower desired limit for accumulator <i>l</i>
<i>MOES</i>	maximum outsourced energy supply
$N_c$	number of steps in control horizon
$N_p$	number of steps in prediction horizon
<i>OES</i>	outsourced energy supply
$P_i^j$	amount of energy or mater per time unit of the flow <i>j</i> that may be produced or consumed by a converter <i>i</i>
<i>PGCC</i>	power grant composite curve
<i>PMS</i>	power management strategy
<i>POW</i>	electrical power
<i>PV</i>	photovoltaic panels
<i>Q</i>	set of all available PMS
<i>RES</i>	renewable energy sources
<i>Rs</i>	set of resources
$SOAcc^l$	state of accumulator <i>l</i>
<i>T</i>	end of time interval
$t_{Lo}$	instant when $SOAcc^l$ reaches the value of the limit <i>Lo</i>
$t_{min}$	instant when $SOAcc^l$ reaches the minimum value of $SOAcc^{l,qk}$ in interval <i>k</i>
$t_0$	beginning of time interval under study
$Up_i^{SOAcc^l}$	upper operating limit for accumulator <i>l</i>
<i>WG</i>	wind generator
<i>WT</i>	water tank
<i>Greek symbols</i>	
$\Delta T$	duration of time interval
$\varepsilon_i(t)$	binary variable that represents the state of converter <i>i</i>
$\rho_i^{SOAcc^l}$	binary variable associated with temporal conditions in accumulator <i>l</i>
<i>Subscripts/superscripts</i>	
<i>Acc</i>	accumulator
<i>Avl</i>	available
<i>Conv</i>	converter
<i>i</i>	index of converter or accumulator
<i>Gen</i>	general
<i>j</i>	flow for a converter or accumulator
<i>k</i>	time interval
<i>l</i>	accumulators as part of the set of Resources
<i>Mat</i>	materials
<i>max</i>	maximum
<i>min</i>	minimum
<i>n, m</i>	resources (converters or accumulators) indicating the type of equipment employed to perform conversion and accumulation tasks $m, n \in Rs, m \neq n$
<i>Nrg</i>	energy

protecting the individual components from malfunctions due to over- or under-utilization. This is clearly a non-trivial task requiring the use of systematic approaches to identify targets of efficient operation which can be subsequently interpreted as appropriately fitted operating realizations.

The recently proposed power Pinch concepts (grand composite curves [1] and composite curves [27]) represent one such approach, allowing the investigation of complex energy systems based on the identification of insights pointing towards optimum decisions. Such methods have been inspired from the well-known heat Pinch [17] and evolved to sophisticated tools [25] that allow for the analysis of complex energy systems [26]. A major advantage of these methods is their implementation in the form of intuitive and easy to develop graphical interfaces (e.g., grand composite curves), whereas the underlying principles are often efficiently represented using rigorous mathematical tools (e.g., flexible process models combined with optimization algorithms). Regardless of the realization, Pinch methods allow the user to easily identify, review, and analyse potentially useful design and operating options [15]. A recent overview of Pinch analysis and mathematical programming for process integration is presented in Ref. [14].

Focusing on electrical systems, Pinch-based analysis methods utilize composite or grand composite curves similarly to the traditional heat Pinch; however, the associated sink and source streams are plotted in power versus time diagrams. In this context, a method proposing the identification of energy recovery targets using the grand composite curves (GCC) analysis approach was reported in Ref. [1] addressing the optimal sizing of power generation systems in the form of an optimization problem. Priya and

Bandyopadhyay [24] also proposed an approach for power systems planning considering a Pinch-based analysis for emissions targeting. Work presented in Ref. [27] proposed the power Pinch analysis (PoPA) method to determine the minimum electricity targets for systems comprising hybrid renewable energy sources. The graphical power Pinch analysis method takes the form of numerical tools in Ref. [20] such as the power cascade analysis (PoCA) and storage cascade table (SCT) in order to facilitate the precise allocation of power and electricity targets in power generation systems. Work presented in Ref. [21] extends the numerical power Pinch method by additionally considering power losses during conversion, transferring, and storage including sizing considerations [28]. The method is applied in the optimization of a pumped hydro-storage system in Ref. [22] that is further extended in Ref. [23] to address the optimal sizing of hybrid power generation systems. Recent work presented in Ref. [29] proposed the outsourced and storage electricity curves (OSEC) to visualize the required minimum outsourced electricity and the current storage capacity at each time interval during startup and operation of hybrid power systems. Methods for load shifting that may lead to further reductions of the maximum storage capacity and the maximum power demand in hybrid systems are also proposed in Ref. [19] using power Pinch analysis, whereas combined load shifting and design is proposed in Ref. [8]. Work presented in Ref. [9] proposed the stand-alone hybrid system, power Pinch analysis method (SAHPPA), which is a graphical tool employing new ways of utilizing the demand and supply through composite curve methods. Recently, work presented in Ref. [10] adapted the power Pinch concept in the electricity system cascade analysis (ESCA) approach to optimise

distributed energy generation systems, while this approach was used for the optimum sizing and operation of a solar/wind/battery hybrid system [30]. The PoPA method has also been transformed into the extended PoPA method [5] to address the design of hybrid systems with battery and hydrogen storage. Mohammad Rozali et al. [18] proposed a power Pinch analysis tool called the AC/DC modified storage cascade to optimise the hybrid power generation systems by considering various storage technologies.

Recently Giaouris et al. [6], exploited the Power Grand Composite Curves (PGCC) approach (originally proposed in Ref. [1], focusing explicitly on the operation of hybrid renewable energy systems with different energy carriers and storage options under the influence of multiple different PMS. The authors showed that multiple Pinch points appear either simultaneously or at different instants when different energy carriers and operating goals are considered. Such points may indicate the energy that needs to be recovered from RES or internal system resources in order to avoid using outsourced electricity from non-RES, the energy that needs to be utilized to avoid overcharging the different storage options and so forth. It was observed that the appearance of multiple Pinch points often resulted in satisfaction of one operating goal at the expense of another (e.g. avoidance of outsourced electricity from non-RES at the expense of battery overcharging). This was addressed through the prioritization of the operating goals that are to be satisfied using the most appropriate PMS from a pool of several alternatives. The selected PMS was the one that resulted in the satisfaction of the primary operating goal and in the smallest possible violation of other secondary goals during a given time interval. This idea was implemented within a framework that exploited the PGCC method to perform two functions: a) the identification of renewable energy recovery targets within a short term prediction horizon, and b) the temporal reallocation of the grid subsystems within a control horizon based on selection of the PMS that best matches the identified targets. The PGCC was therefore exploited for the first time within a model predictive control framework aiming to satisfy the system operating goals. This idea was then tested compared to utilizing a single PMS throughout the system operation and regardless of the available RES, as is mostly the case in commissioned smart grids. The results from exploiting multiple PMS showed a significant reduction in the usage of non-renewable external sources through the recovery of the required energy from internal sources with simultaneous reduction in the utilization of delicate equipment such as the fuel cell (hence reducing the associated wear and tear).

The concept of the PGCC proved very useful in terms of targeting the necessary energy needs. On the other hand, the selection among pre-determined PMS is very useful for practical reasons as the safety and operating limits may be well-tested prior to utilization, offering a predictable system response. However, PMS are essentially pre-determined hierarchical decision structures based on conditions imposed on a sequence of operating parameters that need to be evaluated prior to deciding which sub-system will be activated or deactivated and with what duration [6]. A recent review of various PMS implementations on hybrid energy grids [4] and a more recent work also reviewing several of them [2] indicate that to achieve high system performance it is important to vary both the sequence of evaluation of each parameter and the thresholds of the corresponding conditions. For example, Giaouris et al. [6] developed 9 PMS where the decision structures are combinations of the availability of power from RES, the availability of energy stored in the battery or of hydrogen stored in the tanks and the length of the hysteresis zones (i.e., fixed throughout, variable depending on the time of year or on the duration of activation of each sub-system). Despite the larger number of employed PMS compared to the average of 3 PMS mostly considered in published

literature [3,4], the obtained results indicated that it is necessary to pre-determine a very large number of PMS in order to ensure that no operating constraint is violated and that the energy targets identified from the PGCC may be fully matched and exploited. This is practically difficult because the sub-system interactions represented within a PMS become increasingly complex as more sub-systems are added, whereas the RES behaviour always remains unpredictable.

With very few exceptions, Pinch-based approaches presented to date focus mainly on system sizing. Quite often, the implementation of existing approaches is either illustrated for a few hours (e.g. two days) or for a year using lumped (e.g. monthly) weather data. The consideration of short-term time intervals for wide operating periods is necessary to investigate efficient ways of adapting the system operation under realistic conditions. The use of different power management strategies to change the sequence of activation of different sub-systems and the duration of their operation has received very limited attention as a means of addressing external variability. The appearance of multiple Pinch points in renewable energy systems has been highlighted in a previous work of the authors [6], but the use of pre-specified PMS as a method of adapting the system operation resulted in significant violations of the operating constraints because external variability could not be matched.

To address these challenges this work proposes for the first time an approach which supports the iterative construction of Power Management Strategies (PMS) within short time intervals in the course of system operation by exploiting the Power Grand Composite Curves (PGCC) of the system within a model predictive control (MPC) framework. The proposed approach employs the PGCC for on-line decision making to adapt the system operation to external variability by determining within every time interval the type of converter or accumulator to activate, the instant and duration of the activation and the type and amount of energy carrier to use (i.e. the system PMS). In particular, the PGCC is developed within a prediction horizon of desired duration to identify targets of desired energy utilization and these targets are then satisfied through a PMS that is constructed and implemented for the first time within a control horizon. The simultaneous satisfaction of multiple such targets is an innovative element in the procedure with a beneficial effect on the system performance. Such targets represent important operational goals, which specifically include the avoidance of outsourced energy supply, the avoidance of renewable energy shedding and the ability to develop and maintain desired energy inventories at desired instances. The approach is developed within a formal mathematical framework, which generally refers to conversion and accumulation operations and is independent of the specific system in which it is implemented. It is further illustrated that the adaptive MPC strategy satisfies the desired operating goals under weather conditions that deviate from the available historical data.

## 2. System models and pinch concept

### 2.1. Structural model of motivating system

The system that motivated this work has been constructed and commissioned on location in Greece [12,13] and consists of a LD (local load that needs to be satisfied), PV (photovoltaic panels), a BAT (battery), a FC (fuel cell), an EL (electrolyser), a BF (buffer tank for hydrogen), a CP (compressor), a FT (final tank for hydrogen), a WT (water tank) and a DSL (diesel generator) which is used only as a back-up option. A conceptual flowsheet representing the system as a directed graph is shown in Fig. 1. Regardless of the particular equipment types employed in the

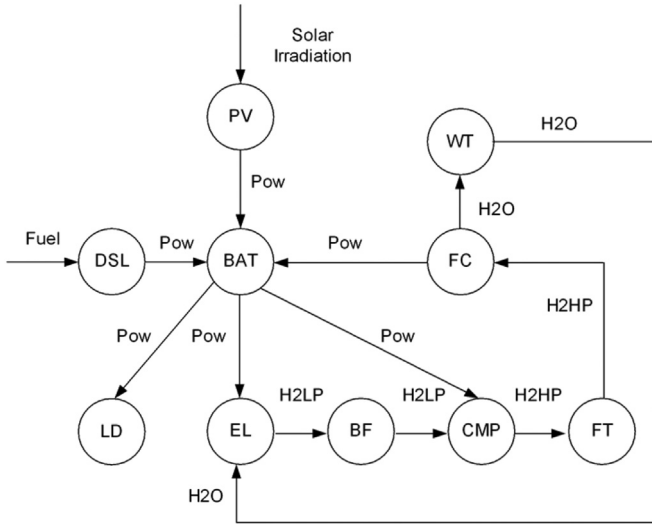


Fig. 1. Conceptual representation of a typical hybrid microgrid with flows as a directed graph.

system of Fig. 1, hybrid RES-based flowsheets may be represented through interconnected converters and accumulators that convert or store material and energy; flows and accumulation at different instants are the key features that drive their operation [7]. The activation instance and operating period of each converter are important operating parameters as they determine their utilization frequency. The state (level) of accumulated energy or materials in the form of diverse energy carriers is also important, prompting the activation of different converters based on their technical characteristics. The duration of activation further depends on a hysteresis based mode of operation, i.e. on whether the converter was active in the previous instant. The combination of these temporal characteristics form complex operating rule sequences called PMS which may be represented through generic models [7].

In this generic context, each device is represented by a node and the edges between the nodes appear when the device is activated. The nodes are classified in two sets, the set of converters ( $Rs^{Conv}$ ) and the set of accumulators ( $Rs^{Acc}$ ). For the system considered in this work these sets contain the following components  $Rs^{Acc} = \{BAT, FT, BF, WT\}$  and  $Rs^{Conv} = \{PV, DSL, EL, FC, CMP\}$ . The connection between two nodes is a flow of either energy (for example electrical in the connection  $FC \rightarrow BAT$ ) or matter (for example hydrogen in the connection  $FT \rightarrow FC$ ). The different types of flow define a set called *Flow* with  $Flow = \{Pow, H2HP, H2LP, H2O\}$ . In this set *Pow* is electrical power, *H2HP* is hydrogen at high pressure stored in the final tank, *H2LP* is hydrogen at low pressure stored in the buffer tank and *H2O* is water stored in the water tank. For this case study an edge is possible to exist only between an accumulator and a converter (and vice-versa), i.e. the connection between two different accumulators is not considered as it can be represented by another accumulator. Based on a similar concept as of that of dynamical systems [16] the state  $S$  of a graph (i.e. of the microgrid) is given by the states of the nodes and edges. These states are variables that fully describe the edges and the nodes, defined as follows:

- For the edges a state must describe its existence, and the type/amount of flow that it contains. This is represented by the variable  $F_{m \rightarrow n}^j(t)$  with  $j \in Flow$  and  $m, n$  two adjacent nodes. When the edge does not exist  $F_{m \rightarrow n}^j(t)$  is zero.

- For accumulators the state is the normalized amount of stored matter or energy, represented by the variable  $SOAcc^l(t) \in [0, 1]$ ,  $l \in Rs^{Acc}$
- For the converters the state is their status (i.e. if they are activated or not) represented by the variable  $\varepsilon_i(t) \in \{0, 1\}$ ,  $i \in Rs^{Conv}$

The state of the graph is therefore fully described as follows:

$$S = \left\{ F_{m \rightarrow n}^j(t), SOAcc^l(t), \varepsilon_i(t) \right\}, l \in Rs^{Acc}, i \in Rs^{Conv}, m, n \in Rs^{Acc} \times Rs^{Conv}, j \in Flow \quad (1)$$

Note that all these states are coupled together (as in typical dynamical systems) because the states of the edges ( $F_{m \rightarrow n}^j(t)$ ) depend on the states of the converters ( $\varepsilon_i(t)$ ), the states of the converters depend on the states of the accumulators ( $SOAcc^l(t)$ ) and the states of the accumulators depend on the state of the edges ( $F_{m \rightarrow n}^j(t)$ )

## 2.2. Temporal model of motivating system

The next step required to fully describe the proposed model is to include the temporal evolution of the state vector  $S$ . For an accumulator  $l$  its state  $SOAcc^l$  is effectively an integrator and it depends on its capacity  $C_l$  and the flows  $F_{m \rightarrow n}^j(t)$  that are directed towards and away from the accumulator:

$$SOAcc^l(t) = SOAcc^l(t-1) + \frac{\sum_{k_1 \in Rs^{Conv}} F_{k_1 \rightarrow l}^j(t) - \sum_{k_2 \in Rs^{Conv}} F_{l \rightarrow k_2}^j(t)}{C_l}, l \in Rs^{Acc}, j \in Flow \quad (2)$$

The state of an edge  $F_{m \rightarrow n}^j(t)$  is defined as follows:

$$F_{m \rightarrow n}^j(t) = \varepsilon_i(t) \cdot P_i^j, i \in \{m, n\}, j \in Flow \quad (3)$$

where  $P_i^j$  is the amount of energy or matter per unit of time that may be converted by the  $i$ -th unit and  $\varepsilon_i$  is the state of the corresponding converter  $i$ . Variables  $P_i^j$  are used as decision parameters and their values are identified by the performed Pinch analysis which is elaborated in the subsequent sections. The Pinch analysis determines the resulting PMS through variable  $\varepsilon_i$  which depends on specific conditions regarding the availability or demand of material or energy in the accumulators. The variable value depends on the following three factors that obtain binary variables [7]:

1.  $\varepsilon_i^{Avl}(t)$  which represents the availability of material or energy that will be converted.
2.  $\varepsilon_i^{Req}(t)$  which represents the demand for material or energy in a conversion.
3.  $\varepsilon_i^{Gen}(t)$  which represent other potentially desired condition(s) that are not associated with the above.

The availability or demand for material or energy to perform a conversion depends on the state of the accumulators. This is quantified through a binary variable  $\rho$  that is 1 when there is availability or demand and 0 otherwise:

$$\begin{aligned} \varepsilon_i^{Avl}(t) &= L^{Avl}_{l \in Rs^{Acc}} \left( \rho_i^{SOAcc^l} \right) \\ \varepsilon_i^{Req}(t) &= L^{Req}_{l \in Rs^{Acc}} \left( \rho_i^{SOAcc^l} \right) \end{aligned} \quad (4)$$

where  $L^{Avl}$  and  $L^{Req}$  are logical operators that are applied on the

variables  $\rho$  which in turn quantify the requirement and the availability of/from the accumulator  $l$ . The general condition can depend on a node or an edge but in most cases it depends on the state of other converters and therefore it can be defined as follows:

$$\varepsilon_i^{Gen}(t) = L_{i \in RS^{Conv}}^{Gen}(\rho_i^l) \quad (5)$$

where again  $L^{Gen}$  is a logical operator. The above are combined into variable  $\varepsilon$  using a logical operator  $L$ :

$$\varepsilon_i(t) = L(\varepsilon_i^{Avl}(t), \varepsilon_i^{Req}(t), \varepsilon_i^{Gen}(t)) \quad (6)$$

To define the variables  $\rho_i^{SOAcc^l}(t)$  we use relational operators applied on the state of various accumulators and predefined variables set again by the PMS. For example see the following expression:

$$\rho_i^{SOAcc^l}(t) = [SOAcc^l(t) < Lo_i^{SOAcc^l}(t)] \quad (7)$$

It implies that the variable  $\rho_i^{SOAcc^l}(t)$  will be 1 if the state of the accumulator  $l$  is less than the variable  $Lo_i^{SOAcc^l}$ . This is a lower ( $Lo$ ) limit in the energy or material available in the accumulator which determines when a converter will be activated. A similar expression may apply for upper limits ( $Up$ ). It has to be mentioned here that in practical applications a hysteresis zone is also used to avoid chattering problems [7]. In our current work we will generate an additional, general structure of conditions that affect the value of the  $\rho$  variables which are independent from the state of the accumulators and enable the derivation of the desired PMS using a Pinch analysis approach based on the PGCC concept.

### 2.3. Example of structural and temporal modelling

In order to elaborate how equations (3)–(7) support the development of a PMS, consider two nodes from the aforementioned energy system, the  $FC$  and the  $BAT$ . The  $FC$  is fed with  $H2HP$  by the  $FT$  and produces  $H2O$  (delivered to the  $WT$ ) and  $Pow$  which is given to the battery. The adjacent edges of the  $FC$  include the edge that connects it to the  $FT$  (the flow is  $H2HP$ ), to the  $WT$  (the flow is  $H2O$ ) and to the battery (the flow is  $Pow$ ); these edges will appear/exist when the  $FC$  is activated. The state of the  $FC$  (i.e. the instant of activation) depends on several conditions which determine the overall PMS. These conditions may be expressed through the variable  $\rho$ . The  $FC$  can therefore be activated when:

1. There is demand for  $Pow$  because the  $BAT$  is not adequately charged, i.e. the  $SOAcc^{BAT}$  is less than a predefined value  $Lo_{FC}^{SOAcc^{BAT}}(t)$ :

$$\rho_{FC}^{SOAcc^{BAT}}(t) = SOAcc^{BAT}(t) < Lo_{FC}^{SOAcc^{BAT}}(t) \quad (8)$$

2. There is availability of hydrogen because the  $FT$  is not empty, i.e. the  $SOAcc^{FT}$  is more than a predefined value  $Lo_{FC}^{SOAcc^{FT}}$ :

$$\rho_{FC}^{SOAcc^{FT}}(t) = SOAcc^{FT}(t) > Lo_{FC}^{SOAcc^{FT}} \quad (9)$$

3. There is available space in the  $WT$  because it is not full, i.e. the  $SOAcc^{WT}$  is less than a predefined value  $Up_{FC}^{SOAcc^{WT}}$ :

$$\rho_{FC}^{SOAcc^{WT}}(t) = SOAcc^{WT}(t) < Up_{FC}^{SOAcc^{WT}}(t) \quad (10)$$

4. The  $DSL$  remains inactive as it was in the previous instant ( $t-1$ ), i.e. there is no reason to activate it if we can use RES to generate the necessary  $Pow$ :

$$\varepsilon_{DSL}(t-1) = 0 \quad (11)$$

The above conditions assume an ON-OFF behaviour without hysteresis. More details regarding the use of a hysteresis zone can be found in Ref. [7]. Conditions (9) and (10) refer to availability and condition (8) refers to demand hence the corresponding superscripts 'Avl' and 'Req' need to be used for the  $\varepsilon$  variables. Condition (11) is a general one which refers to the relation of the  $FC$  with another converter ( $DSL$ ) hence the  $Gen$  superscript needs to be used. Using the appropriate logical operators  $L$  in equations (4)–(6) the equations for the  $\varepsilon$  variables take the following form:

$$\begin{aligned} \varepsilon_{FC}^{Avl}(t) &= \rho_{FC}^{SOAcc^{FT}}(t) \wedge \rho_{FC}^{SOAcc^{WT}}(t) \\ \varepsilon_{FC}^{Req}(t) &= \rho_{FC}^{SOAcc^{BAT}}(t) \\ \varepsilon_{FC}^{Gen}(t) &= [\varepsilon_{DSL}(t-1) = 0] \\ \varepsilon_{FC}(t) &= \varepsilon_{FC}^{Avl}(t) \wedge \varepsilon_{FC}^{Req}(t) \wedge \varepsilon_{FC}^{Gen}(t) \end{aligned} \quad (12)$$

Equations (7)–(12) represent the mathematical expression of the selected PMS and may now be used to calculate the necessary flows around the  $FC$ . For example, based on equation (3) the state of the connection  $FC \rightarrow BAT$  is given by:

$$F_{FC \rightarrow BAT}^{Pow}(t) = \varepsilon_{FC}(t) \cdot P_{FC}^{Pow} = \varepsilon_{FC}(t) \cdot P_{LD}^{Pow} \quad (13)$$

Equation (13) means that the  $FC$  provides the exact amount of power required by the  $LD$ .

### 2.4. Pinch analysis

Apparently, different PMS may result from combinations of logical operators or values imposed on the  $Up$  and  $Lo$  operating limits of equation (7). Each limit represents a practical system operating goal hence it is necessary to select the PMS that allows the system to operate without violating any of the limits. For example, it may be desirable to avoid using the  $DSL$  hence the PMS must be selected that prohibits the state of charge of the battery ( $SOAcc^{BAT}$ ) to drop below a  $Lo$  limit. It may also be desirable to avoid overcharging the battery hence the selected PMS must be the one that prohibits the  $SOAcc^{BAT}$  to climb above an  $Up$  limit. The association of similar limits with the system operating goals has been discussed extensively in Refs. [6,7].

The concept of the Pinch analysis [6] may be used to enable the system operation without violating the corresponding limits. Assume a set  $Q$  of diverse PMS that can be used in a hybrid system within each interval  $k$ , i.e.  $Q = \{PMS_{i,k}, i \in \mathbb{N}\}$ . For any  $PMS_{i,k} \in Q$  the plot of  $SOAcc^l$  vs. time for a range of initial conditions gives the system's PGCC (Fig. 2a). A major requirement in hybrid systems is to avoid the use of outsourced energy supply ( $OES$ ) when  $SOAcc^l$  for any PMS drops below a limit  $Lo$  (e.g., due to insufficient energy in the accumulator, an external source is required to satisfy the load demand). As shown in Fig. 2a even for the same PMS and under the same weather and load demand profiles the PGCC will depend on the value of  $SOAcc^l$  at  $t_0$  and will inevitably result in different  $OES$ . In order to better describe the system state, term  $SOAcc^l$  also receives a

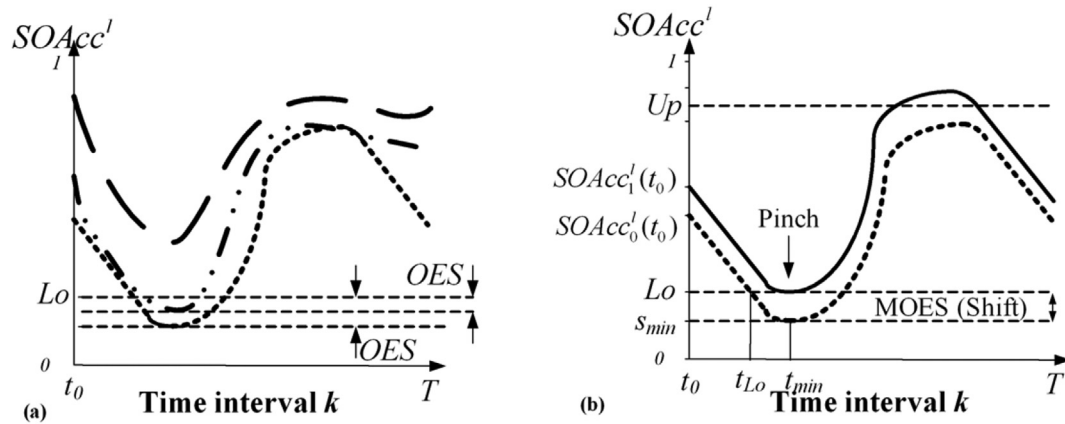


Fig. 2. a) PGCCs for various initial values of  $SOAcc^l$ , b) Shift and Pinch of PGCC.

superscript indicating the shifted level. Finding the PGCC that corresponds to the maximum OES (called MOES) ensures that by covering this energy from RES the system will operate without the use of an outsourced energy supply. Selecting and shifting the PGCC that corresponds to the MOES until it pinches the  $Lo$  limit at  $t_{min}$  (i.e.  $SOAcc^l(t_{min})$ ) indicates the amount of energy required to be available in the accumulator at  $t_0$  (i.e. amount of  $SOAcc^l_2(t_0)$ ) to avoid the use of non-RES (Fig. 2b).

The concepts of the PGCC shift and the Pinch point are clearly very convenient if they are used within a model predictive control framework [6]. Assuming that a time interval with duration 24 h sufficiently describes the system behaviour, a prediction horizon of length 2 intervals (time intervals  $k$  and  $k+1$ ) can be assumed for the satisfaction of the system goals for a selected PMS. A suitable control time horizon of size one time interval (interval  $k$ ) is considered. The control actions involve those decisions about the sequence of equipment utilization and operating patterns in the form of a PMS that satisfy the desired goals. In this context, it is possible to implement a *stored energy targeting step* which essentially involves the identification of the  $SOAcc^l_1(t_0)$  in the prediction horizon ending at  $k+1$  interval based on the procedure described above and depicted in Fig. 2b. Then in a *target matching step* it is possible to compare all the available PMS in the control horizon  $k$  and to identify the one that best matches the target for stored energy  $SOAcc^l_1(t_0)$  identified during the prediction horizon. This will allow the system to have sufficient energy at  $t_0$  in the time interval  $k+1$  so that it will avoid the use of outsourced electricity, assuming that the weather forecast at this interval is sufficiently accurate.

Although the Pinch concept is clearly useful, the utilization of pre-determined PMS includes some challenges. As shown in Fig. 2b it is likely that the shift in the PGCC violates an  $Up$  or other limit which corresponds to an important operating goal (e.g. in case of violation turn off the PV to avoid overcharging the battery), as noted previously in this section. The  $Up$  limit clearly reveals an opportunity to exploit an additional Pinch point (by shifting the PGCC downwards) which will indicate the amount of energy (expressed as  $SOAcc$ ) that needs to be used internally by the system in order to avoid tuning off the PV and hence wasting renewable energy. However, if there is no available PMS that can simultaneously satisfy both limits the only way out is to prioritize the operating goals hence satisfying the one goal at the expense of the others (e.g., avoidance of outsourced electricity from non-RES at the expense of battery overcharging). An additional challenge from using pre-determined PMS is that the desired  $SOAcc^l_1(t_0)$  at interval  $k+1$  may not be exactly matched at the end of interval  $k$  ( $T$ ). The

selection of a PMS that results in  $SOAcc^l(T) > SOAcc^l_1(t_0)$  means that more than the necessary renewable energy is saved during interval  $k$  for the subsequent time interval  $k+1$ , which may have detrimental effects on the system ability to satisfy the LD or on other important operating goals at interval  $k$ . Obviously, the case of  $SOAcc^l(T) < SOAcc^l_1(t_0)$  is ruled out because it does not guarantee the satisfaction of the  $Lo$  limit at interval  $k+1$ . Clearly, the concept of a pool of pre-determined PMS requires the evaluation of a very large number of PMS in order to ensure that no operating constraint is violated and that the energy targets identified from the PGCC may be fully matched and exploited. Although this may be theoretically plausible, it becomes practically challenging because the sub-system interactions represented within a PMS become increasingly complex as more sub-systems are added. Furthermore, the RES behaviour always remains unpredictable hence there is no guarantee that the energy recovery targets identified by Pinch analysis will be matched by the available PMS.

### 3. PGCC shaping

#### 3.1. Basic steps

The proposed approach exploits the PGCC concept together with the previously presented structural and temporal models to develop a new method which does not rely on pre-determined PMS. Instead, the PMS that supports the operation of the hybrid system is determined in the course of the system operation by appropriately shaping a new system PGCC so that multiple operating goals and constraints are satisfied within the same interval. The system PMS is based on a general temporal model which follows a different rationale compared to depending entirely on the state of charge of the accumulator, as in equation (7). This is approached through a procedure consisted of two successive steps which can be used iteratively within multiple time intervals to adapt the system operation under variable environmental conditions:

- The *stored energy targeting step* involves the identification and shifting of the PGCC during the prediction horizon of length one time interval to identify the operational profile of a desired accumulator within this horizon in order to avoid the violation of constraints and satisfy the system operating goals.
- The *target matching step* requires the exact matching of the profile of the shifted PGCC in the control horizon through the automatic formulation of a PMS that exploits converters and accumulators at appropriate time instances.

The proposed approach assumes a system operating within an overall time span  $H$ , divided into equal time intervals (usually 24 h). Each interval is divided into subintervals  $[t_0, T]$  of duration  $\Delta T = T - t_0$  hence for the  $k$ th interval  $t_0 = (k - 1)\Delta T$  and  $T = k\Delta T$ . Subintervals correspond to the time interval used for system simulation purposes. Prediction and control horizons coincide as the dynamics are instantaneous and the effect of the control actions become immediately observed in the system states. The next sections analyse the implementation of the above two steps considering different operating goals.

### 3.2. Avoidance of outsourced electricity supply-Lo type limit

Fig. 3a and b illustrate the two steps through a case that assumes a limit of  $Lo$  type. The operating goal is to avoid obtaining a PGCC that violates the  $Lo$  limit as it signifies a need for outsourced electricity supply (OES), assuming that an accumulator such as a battery is used. It is assumed that the initial value of the  $SOAcc^l$  is at  $SOAcc_0^l(t_0)$ . The *stored energy targeting* step proposes the shifted PGCC (continuous curve in Fig. 2a) which initially indicates the required state of charge of the desired accumulator at  $t_0$  ( $SOAcc_1^l(t_0)$ ) in order to avoid the use of OES. This means that by operating the system starting from  $SOAcc_1^l(t_0)$  instead of  $SOAcc_0^l(t_0)$  the violation of the  $Lo$  limit will be avoided. However, since the  $SOAcc_1^l(t_0)$  is not available at  $t_0$  it is possible to start the operation from  $SOAcc_0^l(t_0)$  and activate a converter which will increase the energy or material level of the accumulator only until the shifted PGCC is reached. In Fig. 3b, the new PGCC of the system will consist of the arrow (activation of a converter) and the dotted-continuous line which coincides with the previously shifted PGCC after  $t_1$ . This new PGCC is the one that should be matched in the *target matching* step through an appropriate PMS.

In Fig. 3a the original PGCC (dashed line) and the shifted PGCC (continuous line) follow the same PMS (determined in a previous interval) with the only difference that they start from a different  $SOAcc^l$  at  $t_0$ . As a result, the only change required to determine a new PMS in Fig. 3b in order to be able to follow the shifted PGCC is the activation of a converter (in this particular case of a  $Lo$  limit). The operation of the converter could last for a minimum  $\Delta t = t_1 - t_0$  if the converter can produce the power or material required to fill the accumulator within this  $\Delta t$ . If the converter has a lower capacity then the charging of the accumulator will last longer.

At this point it is necessary to develop the model that will become the system's PMS. Shifting the PGCC up effectively means

that the system is forced to start at  $SOAcc_1^l(t_0)$  in order to ensure that  $SOAcc_1^l(t_{min}) = Lo$ . The point  $s_{min}$  can be calculated by  $s_{min} = \min_{t \in [t_0, T]} (SOAcc_0^l(t))$  hence:

$$SOAcc_1^l(t_0) = Lo - s_{min} + SOAcc_0^l(t_0) \quad (14)$$

The key idea is that if energy is provided by an appropriate converter to the system that starts from  $SOAcc_0^l(t_0)$  such that  $SOAcc_0^l(t_1) = SOAcc_1^l(t_1)$ , then without further use of this converter (or outsourced energy supply) the  $Lo$  limit will not be violated. The appropriate amount of energy  $E$  (kWh) that must be provided by the converter  $i$  is calculated by:

$$E_i = C_i \cdot (Lo - s_{min}) \quad (15)$$

Hence, the variable  $\rho_i^{SOAcc^l}(t)$  (the condition in order to initiate the required converter and provide the necessary flow) defined in equation (7) is equal to:

$$\rho_i^{SOAcc^l}(t) = \begin{cases} 1, & t = t_0 \\ 0, & \text{Otherwise} \end{cases} \quad (16)$$

Note that the use of equation (16) is independent of the state of charge of the accumulator. As an example of the aforementioned analysis, assume that the accumulator  $l$  is the *BAT*. The *FC* is a converter that may be used in this case in order to develop the overall PMS. By injecting power from the *FC* to the system it is possible to reach the desired  $SOAcc_1^l(t_1)$  hence avoiding the violation of the  $Lo$  limit and the utilization of the *DSL*. Instead of using equation (8) the system PMS around the *FC* and associated calculations will be performed as follows:

$$\begin{aligned} \rho^{SOAcc^{BAT,FC}}(t) &= \begin{cases} 1, & t = 1 \\ 0, & \text{Otherwise} \end{cases} \\ F_{FC \rightarrow BAT}^{Pow}(t) &= \varepsilon_{FC}(t) \cdot P_{FC}^{Pow} \\ E_{FC} &= C_{BAT} \cdot (Lo - s_{min}) \\ \rho_{FC}^{SOAcc^{FT}}(t) &= SOAcc^{FT}(t) > Lo_{FC}^{SOAcc^{FT}}(t) \\ \rho_{FC}^{SOAcc^{WT}}(t) &= SOAcc^{WT}(t) < Up_{FC}^{SOAcc^{WT}}(t) \\ \varepsilon_{DSL}(t - 1) &= 0 \end{aligned} \quad (17)$$

The full set of equations that define a generic structure of the PMS around all the other accumulators and converters is given in the Appendix for this and the subsequently investigated cases. Notice that the state of the connection  $F_{FC \rightarrow BAT}^{Pow}(t)$  is different to that of equation (13), which depends on the extent of shift that is

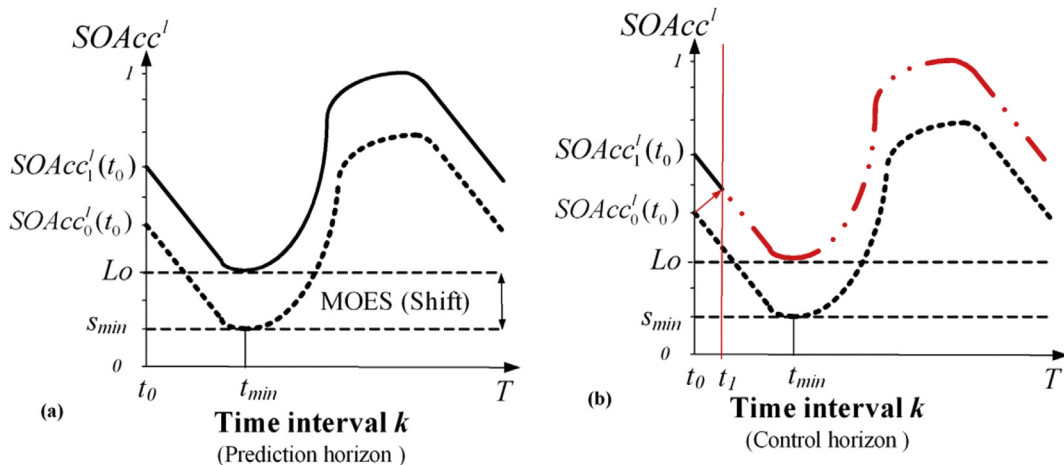


Fig. 3. a) Original (dashed line) and shifted (continuous line) system PGCC, b) Activation of a converter (red arrow) to follow the shifted PGCC (dashed-double dotted line is desired part of the shifted PGCC). (For interpretation of the references to colour in this figure legend, the reader is referred to the web version of this article.)

required. Note that if the power (kW) required from the FC is higher than the maximum power that it can provide ( $P_{FC}^{Max}$ ), then the induced power will be  $P_{FC}^{Max}$  but the injection will last for  $[E_{FC}/P_{FC}^{Max}]$  hours so that  $SOAcc_0^{BAT}([E_{FC}/P_{FC}^{Max}]) = SOAcc_1^{BAT}([E_{FC}/P_{FC}^{Max}])$ . Without loss of generality and in order to facilitate the elaboration of the proposed concepts it will be assumed that within 1 h the FC can provide all the demanded energy. Hence in equation (17)  $P_{FC}^{Pow}$  equals to  $E_{FC}$  divided by 1 h. Note that the proposed approach also supports different cases where the FC may operate as long as required.

### 3.3. Avoidance of overcharging and outsourced electricity supply-Lo and Up type limits

The Up type limit may correspond to conditions where a converter must be deactivated for reasons of safety or protection of other equipment. For example, it may correspond to the undesired but necessary deactivation of the PV to protect the BAT from overcharging at the expense of wasting renewable energy in conditions of high solar radiation. The violation of an Up limit is addressed through the PGCC approach by a downward shift until the PGCC pinches the Up limit [6]. When the two limits co-exist, the upward (in a Lo limit) or downward (in an Up limit) shift in the PGCC may result in the satisfaction of one of them but it may also result in violation of the other. Based on the proposed method, this situation may be avoided as follows:

- By performing two successive, separate shifts in the stored energy targeting step; first in the original PGCC (Fig. 4a) and then in the shifted PGCC (Fig. 4b) hence finding the pinch points in both limits.
- By matching the two separate profiles of the PGCC through the initiation of the necessary converters (Fig. 5a and b); these actions will form the new PMS.

Fig. 4 describes the actions in the stored energy targeting step. In Fig. 4a the shift is implemented as described in the previous section to find Pinch<sub>1</sub> at the Lo limit, disregarding the violation of the Up limit. Fig. 4b serves to find Pinch<sub>2</sub>. The instant  $t_{up}$  is identified at the point where the shifted PGCC (continuous black line) violates for the first time the Up limit and then only the part of the shifted PGCC after  $t_{up}$  is shifted down in order to identify Pinch<sub>2</sub>.

Fig. 5 describes the actions in the target matching step. Fig. 5a

indicates the procedure that is described in the previous section regarding the new PMS. A converter is initiated from  $t_0$  until  $t_1$  which will increase the energy or material level of the accumulator until the shifted PGCC is reached. This PGCC will indicate the instant  $t_{up}$ , when the accumulator exceeds the Up limit. The PMS that represents the shifted PGCC will be followed until instant  $t_{up} - 1$  which is selected as one subinterval (or as many as required) away from  $t_{up}$  in order to initiate a control action which will avoid the violation of the Up limit. Fig. 5b indicates the procedure after  $t_{up} - 1$ . At  $t_{up} - 1$  a new converter will be activated (arrow between  $t_{up} - 1$  and  $t_{up}$ ) which will discharge the accumulator enough (i.e., reduce the  $SOAcc^l$ ) so that the curve resulting from the second shift (Pinch<sub>2</sub> at the Up limit of Fig. 4b) may be followed in order to avoid violation of the Up limit. Note here that the activation of the converter that will discharge the corresponding accumulator may be implemented anytime between  $t_{min}$  and  $t_{up} - 1$ . The overall PGCC will have a completely new shape as it will be a composite of the two arrows and the two red lines (dashed line with double dots until  $t_{up} - 1$  and dashed line with single dot after that).

The development of a model for the representation of the composite PGCC of Fig. 5b through a PMS is based on equations (15) and (16). Assuming that the converter utilized in this case is the EL its activation will be based on the following rule:

$$\begin{aligned} \rho_{EL}^{SOAcc^{BAT}}(t) &= \begin{cases} 1, & t = t_{up} - 1 \\ 0, & \text{otherwise} \end{cases} \\ E_{EL} &= C_{BAT} \cdot (s_{max} - Up) \\ \rho_{EL}^{SOAcc^{WT}}(t) &= SOAcc^{WT}(t) > Lo_{EL \rightarrow BF}^{SOAcc^{WT}}(t) \\ \rho_{EL}^{SOAcc^{BF}}(t) &= SOAcc^{BF}(t) < Up_{EL \rightarrow BF}^{SOAcc^{BF}}(t) \\ \varepsilon_{EL}^{Avt}(t) &= \rho_{EL \rightarrow BF}^{SOAcc^{BAT}}(t) \wedge \rho_{EL \rightarrow BF}^{SOAcc^{WT}}(t) \\ \varepsilon_{EL}^{Req}(t) &= \rho_{EL \rightarrow BF}^{SOAcc^{BF}}(t) \\ \varepsilon_{EL}^{Gen}(t) &= 1 \\ \varepsilon_{EL}(t) &= \varepsilon_{EL \rightarrow BF}^{Avt}(t) \wedge \varepsilon_{EL \rightarrow BF}^{Req}(t) \wedge \varepsilon_{EL \rightarrow BF}^{Gen}(t) \\ F_{BAT \rightarrow EL}^{Pow}(t) &= \varepsilon_{EL}(t) \cdot P_{EL}^{Pow} \end{aligned} \quad (18)$$

$$\text{where } Up = SOAcc_2^{BAT}(t_{max}) \text{ and } s_{max} = \max_{t \in [t_0, T]}(SOAcc_1^{BAT}(t)).$$

### 3.4. Returning to the initial state of charge-Lo, Up and End type limits

A desired condition in such systems may be to achieve a full cycle in the charging–discharging process of an accumulator in the

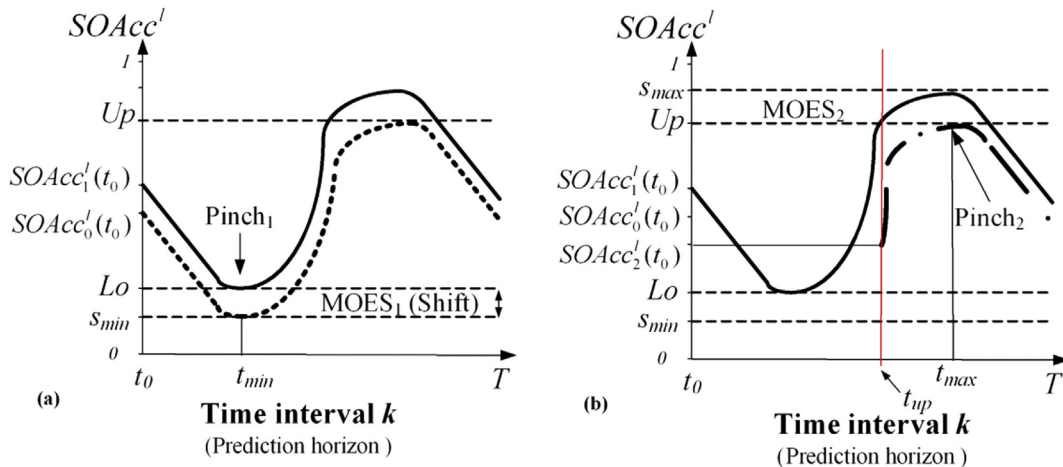
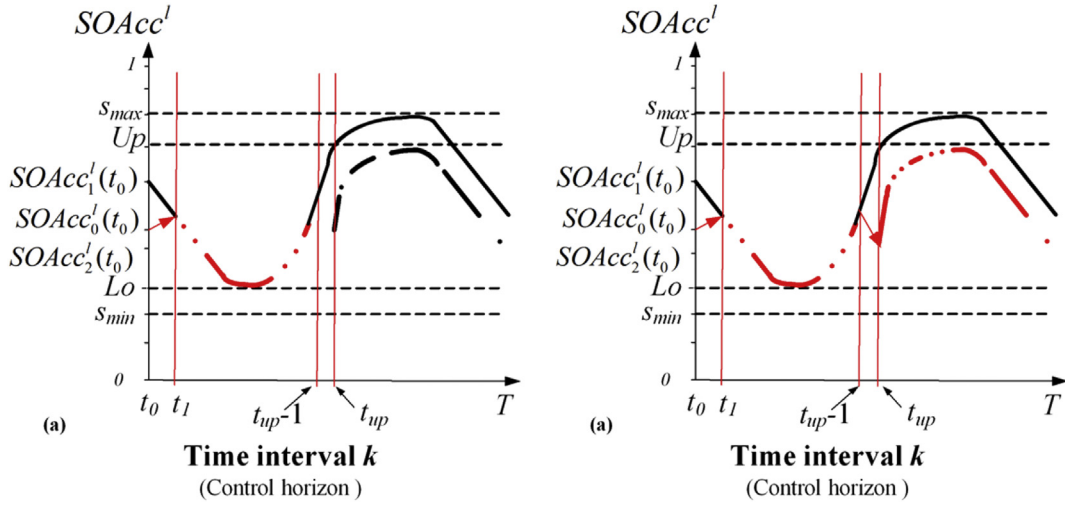


Fig. 4. a) The first shift of the PGCC starting from  $SOAcc_1^l(t_0)$  serves to identify Pinch<sub>1</sub> and avoid the Lo limit (the dashed line is the original PGCC and the continuous is the shifted PGCC), b) The second shift of the PGCC starting from  $SOAcc_1^l(t_0)$  after instant  $t_{up}$  serves to identify Pinch<sub>2</sub> and avoid the Up limit (the dashed-dotted line is the shifted PGCC in this case).



**Fig. 5.** a) A converter is activated between  $t_0$  and  $t_1$  to charge the accumulator until the shifted PGCC starting from  $SOAcc^l_1(t_0)$  and the shifted PGCC is followed until  $t_{up} - 1$  (the arrow and dashed-double dotted line are the desired parts of the PGCC), b) a converter is activated between  $t_{up} - 1$  and  $t_{up}$  until the shifted PGCC (dashed-dotted line) which is then followed (the new arrow and the dashed-double dotted line are the desired parts of the PGCC).

end of a time interval. The concept is illustrated in Fig. 6. This means that in the end of the current interval the state of charge of the accumulator ( $SOAcc$ ) should be the same as in the beginning of the interval hence  $SOAcc^l_2(t_0) = SOAcc^l_2(T - 1)$ . Note that the interval end is defined as the instant when the  $SOAcc$  is last checked, hence the  $T-1$ . Such an example is the case of a  $BAT$  where a 24 h interval is assumed with a subinterval of 1 h and it is important to achieve  $SOAcc^{BAT}_2(00:00) = SOAcc^{BAT}_2(23:00)$  (i.e.,  $T = 23:00$  h). If  $SOAcc^{BAT}_2(00:00) > SOAcc^{BAT}_2(23:00)$  then the  $BAT$  will end up discharged and it may result in the future activation of the  $DSL$ . If  $SOAcc^{BAT}_2(00:00) < SOAcc^{BAT}_2(23:00)$  then the  $BAT$  contains excess energy that may be transformed and stored as hydrogen. This is achieved by directly activating a converter such as the  $FC$  at instant  $T-1$  (i.e. at  $t = 22:00$  h). The activation takes place at the end of the control horizon. In case that it is necessary to discharge the  $BAT$  and produce hydrogen through the operation of the  $EL$ .

To develop a model for the PMS, the energy that must be provided in Fig. 6 (or removed in a similar case) should be equal to  $|\Delta S| \cdot C_{BAT}$ , where  $\Delta S = SOAcc^l_2(t_0) - SOAcc^l_2(T - 1)$ . Considering that the  $FC$  will be used in a case of charging and the  $EL$  in the case of discharging the overall equations will take the following form:

$$\rho_{FC}^{SOAcc^{BAT}}(t) = \begin{cases} 1, & [t = t_0] \vee [t = T - 1 \wedge \Delta S < 0] \\ 0, & \text{Otherwise} \end{cases} \quad (19)$$

$$\rho_{EL}^{SOAcc^{BAT}}(t) = \begin{cases} 1, & [t = t_{up} - 1] \vee [t = T - 1 \wedge \Delta S > 0] \\ 0, & \text{Otherwise} \end{cases} \quad (20)$$

$$E_{FC} = \begin{cases} C_{BAT} \cdot (Lo - s_{min}) & [t = t_0] \wedge [Lo > s_{min}] \\ |\Delta S| \cdot C_{BAT} & [t = T - 1] \wedge [\Delta S < 0] \\ 0 & \text{Otherwise} \end{cases} \quad (21)$$

$$E_{EL} = \begin{cases} C_{BAT} \cdot (s_{max} - Up) & [t = t_{up} - 1] \wedge [Up < s_{max}] \\ |\Delta S| \cdot C_{BAT} & [t = T - 1] \wedge [\Delta S < 0] \\ 0 & \text{Otherwise} \end{cases} \quad (22)$$

$$\begin{aligned} F_{BAT \rightarrow EL}^{Pow}(t) &= \varepsilon_{EL}(t) \cdot P_{EL}^{Pow} \\ F_{FC \rightarrow BAT}^{Pow}(t) &= \varepsilon_{FC}(t) \cdot P_{FC}^{Pow} \end{aligned} \quad (23)$$

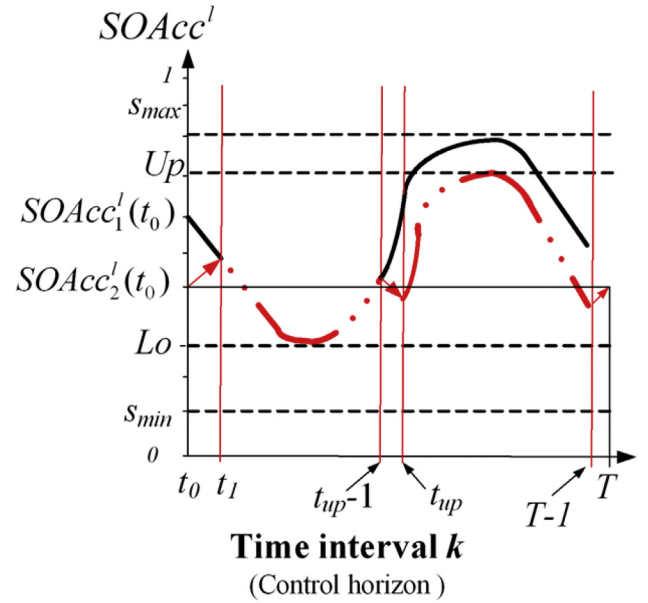


**Fig. 6.** An appropriate converter is activated so that in the end of this interval the state of charge of the accumulator ( $SOAcc$ ) becomes the same as in the beginning of the interval.

### 3.5. Algorithmic implementation

The aim of the previous section was to present the main features of the proposed approach as a graphical method. This section presents the approach in the form of algorithmic steps that can be implemented in order to automate the calculations. The proposed algorithm refers to several of the equations reported in the previous section in a more general form. The algorithm is generally intended to be used for multiple time intervals, where the implementation of the graphical approach may be tedious. A graphical analysis of the system for few time intervals should always be performed prior to using the algorithm so that the user may properly adjust different algorithmic parameters based on the specifics of the problem at hand. The proposed steps are detailed below and summarized in Fig. 7:

1. Specify an overall time span, a number of intervals and a prediction and control horizon.
2. Specify an initial PMS structure and the system state from equation (1).
3. Select an accumulator  $l$  from  $Rs^{Acc}$  and determine limits  $Lo$ ,  $Up$ ,  $End$ .
4. At interval  $k$ , starting from  $SOAcc_0^l(t_0)$  calculate the system PGCC using equations (2)–(7):
5. Calculate  $s_{min} = \min_{t \in [t_0, T]} (SOAcc_0^l(t))$  and  $s_{max} = \max_{t \in [t_0, T]} (SOAcc_0^l(t))$ 
  - 5.1 If  $s_{min} < Lo$  then:
    - 5.1.1 In the prediction horizon:
      - a. Specify  $t_1 = t_0 + \Delta t$ , setting a desired value for  $\Delta t$ .
      - b. Calculate  $SOAcc_1^l(t_1) = SOAcc_0^l(t_1) + Lo - s_{min}$  (the PGCC is shifted up by  $Lo - s_{min}$ ).
      - c. Calculate from equation (15) the energy  $E$  needed to match  $SOAcc_1^l(t_1)$  starting from  $SOAcc_0^l(t_0)$ .
    - 5.1.2 In the control horizon:
      - a. Select the converter  $i$  from  $Rs^{Conv}$  that will provide energy  $E$ .
      - b. Activate converter  $i$  at  $t_0$  based on equation (17).
  - 5.1.3 If  $SOAcc_1^l(t_1)$  is matched by converter  $i$  then go to step 5.2, else increase  $\Delta t$  and go to step 5.1.1a.
- 5.2 If  $s_{max} > Up$  for either the original or the shifted PGCC then:
  - 5.2.1 In the prediction horizon:
    - a. Set  $t_{up}$  as the instant where the condition of step 5.2 occurs and specify a  $\Delta t$ .
    - b. Calculate  $SOAcc_2^l(t_{up}) = SOAcc_1^l(t_{up}) + s_{max} - Up$  (the PGCC is shifted down by  $s_{max} - Up$ ).
    - c. Calculate from equation (18) the energy  $E$  needed to match  $SOAcc_2^l(t_{up})$  starting from  $SOAcc_1^l(t_{up} - \Delta t)$  (or by setting  $s_{max} - Up$  in equation (15)).
  - 5.2.2 In the control horizon:
    - a. Select the converter  $i$  from  $Rs^{Conv}$  that will provide energy  $E$ .
    - b. Activate converter  $i$  at  $t_{up} - \Delta t$  based on equation (18).
  - 5.2.3 If  $SOAcc_2^l(t_{up})$  is matched by converter  $i$  then go to step 6, else increase  $\Delta t$  and go to step 5.2.1a.
6. Calculate  $SOAcc_0^l(T-1)$  or  $SOAcc_1^l(T-1)$  or  $SOAcc_2^l(T-1)$  if the previous step was 5., 5.1 or 5.2, respectively.
  - 6.1 If  $SOAcc_{cs}^l(T-1) \neq SOAcc_{cs}^l(t_0)$  ( $cs = 0$  or  $1$  or  $2$ ) then:
    - 6.1.1 In the prediction horizon:
      - a. Calculate  $\Delta S = SOAcc_{cs}^l(t_0) - SOAcc_{cs}^l(T-1)$  ( $cs = 0$  or  $1$  or  $2$ ).
      - b. Calculate from equation (21) or (22) the energy  $E$  needed to match  $SOAcc_{cs}^l(t_0)$  at  $T$ , depending on whether  $\Delta S < 0$  or  $\Delta S > 0$ .
    - 6.1.2 In the control horizon:
      - a. Select the converter  $i$  from  $Rs^{Conv}$  that will provide energy  $E$  at  $T-1$ , depending on whether  $\Delta S < 0$  or  $\Delta S > 0$ .
      - b. Activate converter  $i$  at  $T-1$  based on equation (19) or (20) and calculate the corresponding flows based on equation (23), depending on whether  $\Delta S < 0$  or  $\Delta S > 0$ .
7. Set the next time interval as the current interval  $k$ , the PMS of the previous interval as the current initial PMS and  $SOAcc_0^l(t_0) = SOAcc_{cs}^l(T)$  ( $cs = 0$  or  $1$  or  $2$ ).
8. Repeat from step 4 until the end of the selected time span.

Note that several equations presented in the previous sections assume a  $BAT$  as the accumulator, but the same concept can also be applied for accumulators of different types that may handle other energy carriers. Step 5.1.2b refers to equation (17) assuming any converter type that will have a similar effect as an  $FC$ . Although more generic equations were provided prior to equation (17), this

equation is selected because it also includes the flows that need to be adjusted in this case, as well as all other variables that are affected and act as constraints that must be satisfied in order for the converter to be activated. Also note that equation (17) assumes  $\Delta t = 1$ , although a different value may also be considered. The same holds with respect to the variables, flows, constraints and  $\Delta t$  with respect to equation (18) in step 5.2. In the case of step 6 which refers to the  $End$  limit, the equations used consider simultaneously that both limits  $Lo$  and  $Up$  have been violated. The algorithm proposed here addresses these limits before step 6 hence equations (19)–(22) should be applied without the terms associated to the previous steps. Finally, note that the actions performed in the control horizon include the selection of a converter as a first step. Although more than one converters can be used in principle to perform the same task (e.g. of charging or discharging), in this work we only consider one converter every time because in the considered system there is always only one option that inherently satisfies operating constraints. For example, charging is performed using the  $FC$  because the  $DSL$  represents an outsourced electricity supply option and is automatically eliminated. However, if there is more than one available converters that meet the operating requirements, their selection may be based on specific criteria (e.g., economic) evaluated on-line during the implementation of the algorithm. Furthermore, converters may be prioritized beforehand based on the system analysis using the graphical tools and selected hierarchically during the system operation. Such options are directly supported by the presented model predictive control formulation and general PMS structure.

#### 4. Implementation

The proposed developments will be illustrated in case studies where the system PMS is developed using the  $FC$  and the  $EL$  as the converters which are initiated to match the desired PGCC. The  $DSL$  is also used as a back-up option. The first case study illustrates important features of the method within a 24 h interval. The second case study considers two cases. Firstly, yearly historical weather data are employed to emulate an accurate (ideal) forecast and demonstrate the implementation of the proposed approach. In the second case random variations obtained from a normal distribution are imposed on the historical weather data, to emulate the weather unpredictability and investigate the performance of the proposed approach under realistic operating conditions (i.e., predicted and actual weather conditions do not match). The system is simulated for a 24 h time interval  $k$  within a yearly horizon, using averaged hourly weather data. It is therefore assumed that  $t_0 = 00:00$  and  $T = 23:00$  at every interval. The  $LD$  is assumed constant at 1.5 kW, the employed RES is the PV and the  $BAT$  capacity is  $C_{BAT} = 144$  kW. Note that the method may also be implemented for a variable  $LD$  demand and other RES. Specific technical system characteristics are obtained from Ref. [7]. It is assumed that the system is activated in January 1st with the following initial state status:  $SOAcc_0^{BAT}(00:00) = 0.25$ ,  $SOAcc_0^{FT}(00:00) = 0.8$ ,  $SOAcc_0^{BF}(00:00) = 0.5$ ,  $SOAcc_0^{WT}(00:00) = 0.7$ ,  $\varepsilon_{PV}(00:00) = 1$ ,  $\varepsilon_i(00:00) = 1 \forall i \in Rs^{Conv}$ , excluding the connections between PV and BAT as well as BAT and LD. The  $Lo$  limit is set at  $SOAcc^{BAT} = 0.2$  (i.e.,  $Lo = 0.2$ ), the  $Up$  limit at  $SOAcc^{BAT} = 0.8$  (i.e.,  $Up = 0.8$ ) and the  $End$  limit condition is that  $SOAcc_0^l(00:00) = SOAcc_0^l(23:00)$

#### 5. Results and discussion

##### 5.1. Illustration of the proposed approach

The daily power delivered by the PV is shown in Fig. 8a whereas the PGCC for the initial conditions is shown in Fig. 8b (blue solid

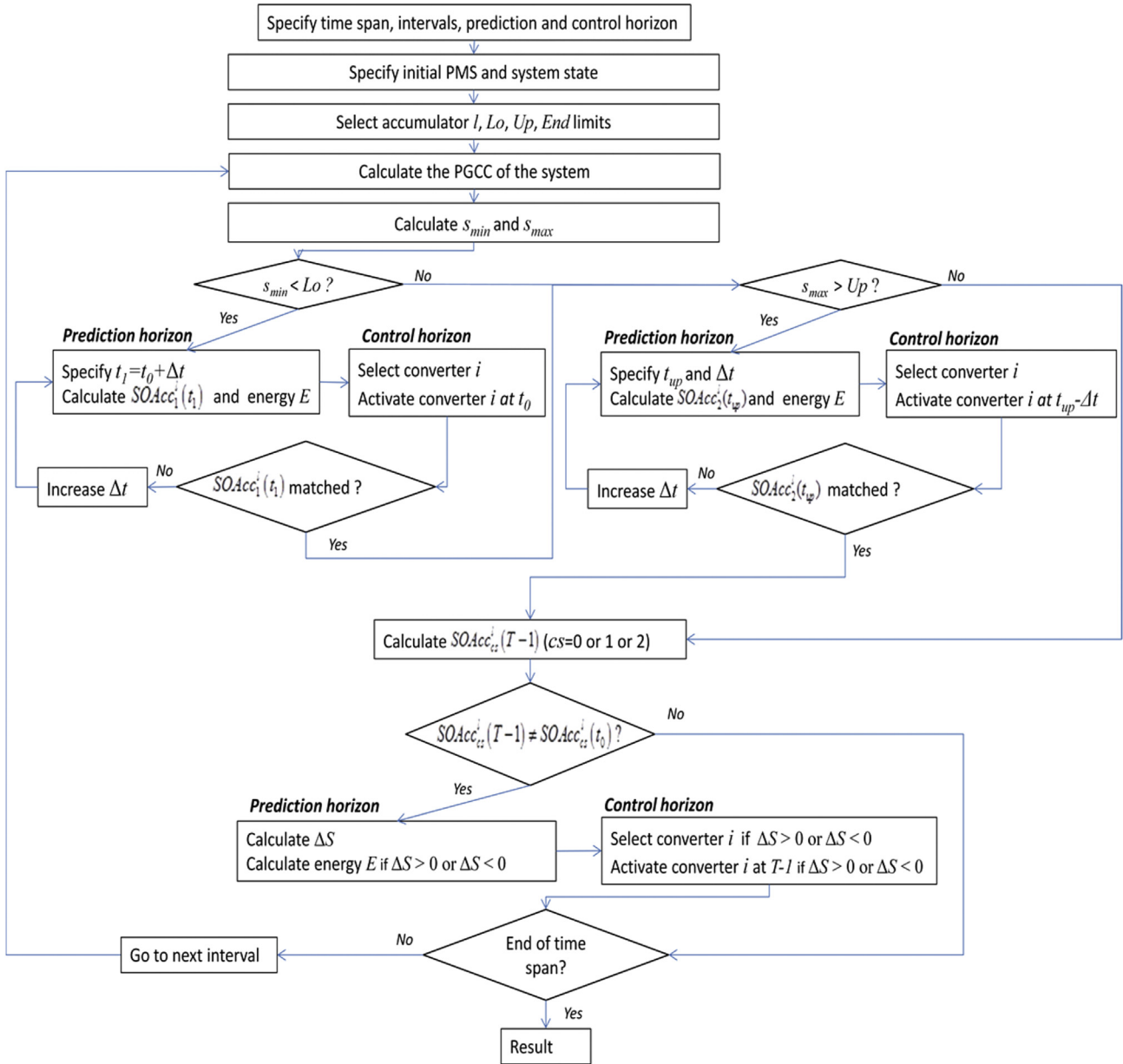


Fig. 7. Conceptual information flow diagram of proposed algorithmic steps.

line). The minimum value of the system PGCC is  $s_{min} = 0.1581$  and the required shift is  $Lo - s_{min} = 0.0419$ . From equation (14) the shifted PGCC (dots of Fig. 7b) will be at  $SOAcc_1^{BAT}(00 : 00) = 0.2919$  and as expected it presents a pinch at the value of 0.2. The minimum outsourced electricity supply required by the system is given by the shifted curve at 0.0491. This implies that the power required by the FC at  $t_0 = 00:00$  is  $P_{FC}^{pow} = 0.0491 \cdot 144 = 7.07$  kW based on equation (15). Fig. 8b shows the new PGCC (red solid line) response when the desired amount of power is provided by the FC for 1 h.

The  $Up$  limit is addressed by first noticing that the shifted PGCC (which aimed at avoiding the  $Lo$  limit in Fig. 8b) has  $s_{max} = 0.9138$ , i.e. the required shift is  $Up - s_{max} = 0.1138$ . Based on the availability of hourly weather data that is assumed here, the first time where a sample is higher than this limit is at  $t_{up} = 16:00$ . Hence, the amount of energy that must be consumed by the EL is  $P_{EL}^{pow} = 0.1138 \times 144 = 16.38$  kW and it will be activated at  $t_{up} - 1 = 15:00$ . Fig. 9 shows the response of the system when it

violates the  $Up$  limit (blue line) and with the correction when the EL is activated at 15:00 (red line).

The last condition associated with the  $End$  type limit, i.e. that  $\Delta S = SOAcc^l(t_0) - SOAcc^l(T - 1) = 0$ , is investigated using the EL in this case to produce hydrogen. Fig. 10 shows that the last value of the PGCC one time sample before the end of the time interval at  $T - 1 = 22:00$  is  $SOAcc^{BAT}(23:00) = 0.7443$ . Hence  $\Delta S = 0.7443 - 0.25 = 0.4943$  and therefore at  $t = 23:00$  the EL must be activated in order to remove  $0.4943 \times 144 = 71.18$  kW and produce the corresponding hydrogen. If more power is required than the maximum that the EL can consume (in this case of 71 kWh) then the EL can be activated for a longer duration as long as the consumed energy forces  $\Delta S = 0$ . Fig. 9 shows that indeed by activating the EL at  $t = 21:00$  for 2 h we have that  $SOAcc^{BAT}(00 : 00) = SOAcc^{BAT}(24 : 00)$  which proves that the PGCC can be completely shaped according to practically any design restriction. The changes in the system operation are implemented

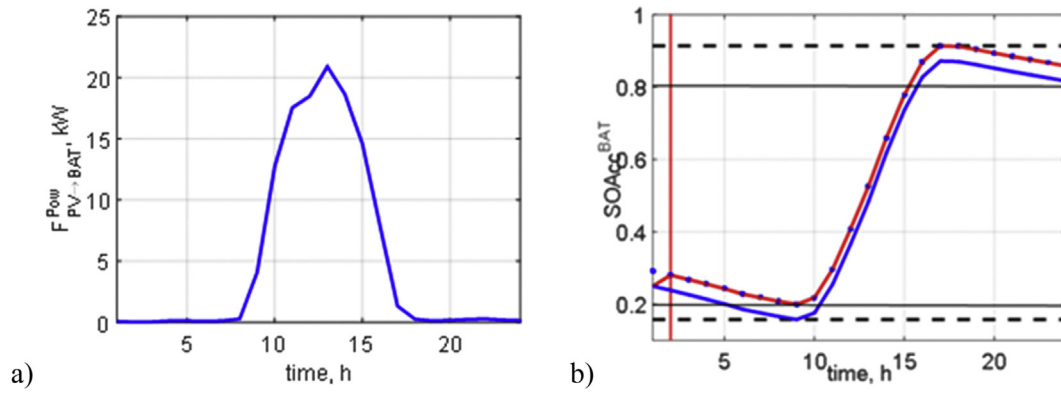


**Fig. 8.** a) Daily power profile delivered from the PV, b) The system PGCC (blue solid line), the system shifted PGCC (dots) and the new PGCC after initiation of the FC to avoid the  $Lo$  limit (red solid line). The intensely dashed lines indicate the  $s_{min}$  and  $s_{max}$ . (For interpretation of the references to colour in this figure legend, the reader is referred to the web version of this article.)

through the PMS that are developed in the course and as a result of the PGCC shaping.

## 5.2. Year-round operation

### 5.2.1. Ideal weather forecasting

To further investigate the proposed approach, the yearly operation of the system is investigated under again ideal weather forecasting. As ideal weather conditions are used, the main issue that needs to be investigated is the performance of the system for different values of the limit  $Lo$ ,  $Up$  and  $End$ . Fig. 11 shows the response of the system when the operational limits are  $Lo = 0.3$ ,  $Up = 0.7$  and the initial  $SOAcc^{BAT}(00:00)$  takes the following values 0.69, 0.6, 0.5, 0.4 and 0.31. These values were chosen as indicative for possible combinations of the three limits. We will investigate if there is a violation of the  $Up$ ,  $Lo$  and  $End$  limits within the year and if there are combinations of limit values that result in violations.

From the above figures we can see the possible responses when the three limits take different values. As expected in most cases all three limits are satisfied apart from the extreme cases (Fig. 11a and e). A key factor here is the capacity of  $SOAcc^{FT}$ , as when the

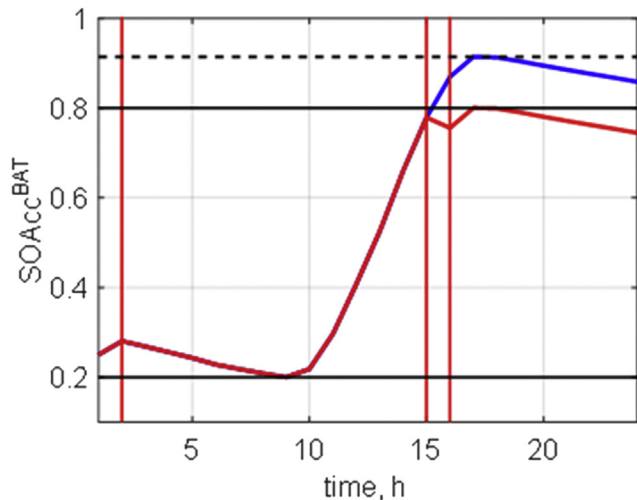


**Fig. 9.** The new PGCC after initiation of the FC to avoid the  $Lo$  limit (red line until 15:00 and blue line after that), the PGCC of the initiated EL between 15:00 and 16:00 and the new downward shift in the PGCC after 16:00 (red line after 16:00). (For interpretation of the references to colour in this figure legend, the reader is referred to the web version of this article.)

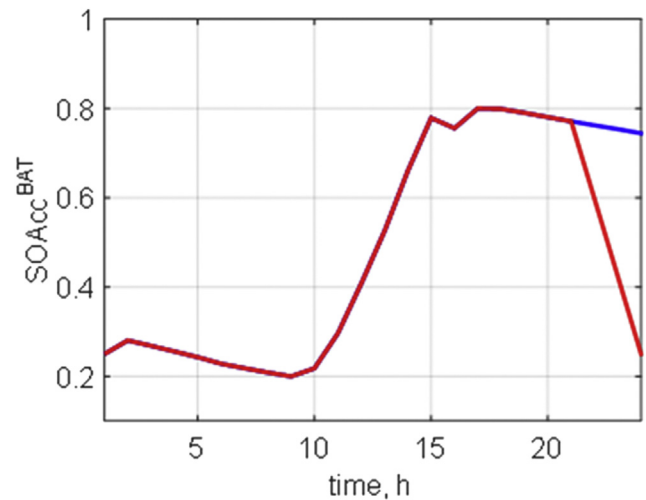


**Fig. 10.** Discharge of the BAT after 21:00 using the EL to meet the  $End$  type limit. The blue trace is the PGCC that resulted after the 2nd shift and the red trace is the PGCC that includes all three shifts. (For interpretation of the references to colour in this figure legend, the reader is referred to the web version of this article.)

$End = 0.31$  and  $Lo = 0.3$  limits are close (one type of extreme case in Fig. 11e) then the FC has to be frequently used. This is happening because if the system starts at 00:00 close to the  $Lo$  limit (which was a result of the previous day  $End$  limit) due to the lack of power produced from the PV the  $SOAcc^{BAT}$  will drop and hence the FC must be activated. Another interesting phenomenon is observed in the other extreme case (Fig. 11a), where the  $End$  limit is very close to the  $Up$  limit, i.e. at the start of each day we have a charged battery. In this case the  $Lo$  limit is also violated but for a different reason. This is happening because during the summer the solar irradiation is high and hence as the system starts from a very high value the estimated  $SOAcc^{BAT}$  becomes greater than 1. This results in an estimated power consumption by the EL greater than 57.6 kW which is the maximum that should be removed in the zone 0.7 to 0.3 (as  $0.7 - 0.3 = 0.4$  and  $0.4 \times 144 \text{ kW} = 57.6 \text{ kW}$ ). Obviously, this can be altered if the maximum value of the power consumed by the EL is  $(Up - Lo) \times 144 \text{ kW}$  but then the  $Up$  limit will be violated as not enough power is consumed. In Fig. 11b,c,d where the difference between the limits is higher than 0.1 the system operates within the desired constraints throughout the year as the PGCC is continuously shaped according to the available renewable energy and LD demands.

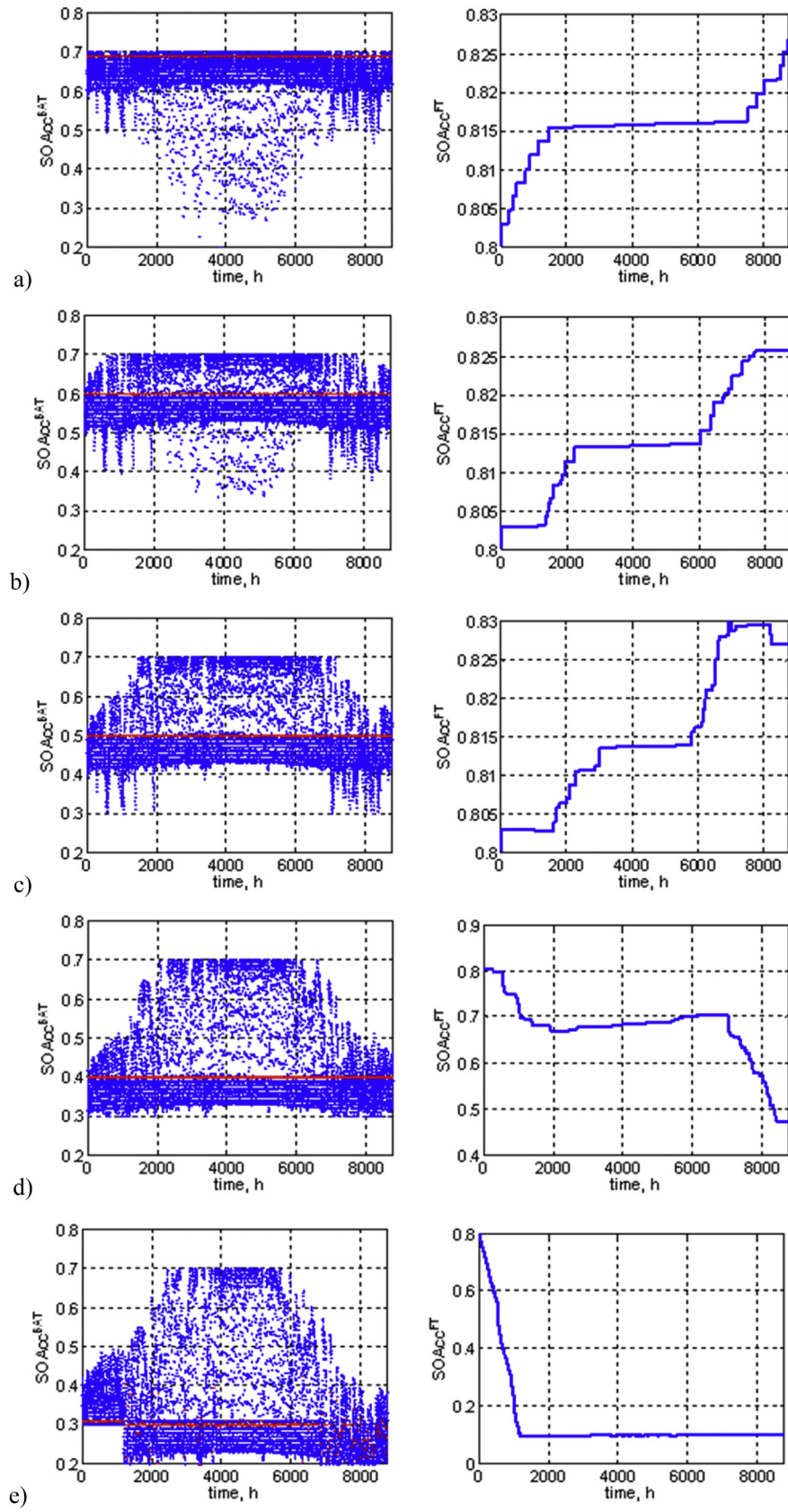


**Fig. 11.** Year round system response for ideal weather forecasting and the initial  $SOAcc^{BAT}(00:00)$  at a) 0.69, b) 0.6, c) 0.5, d) 0.4, e) 0.31. The left side diagrams show the responses of  $SOAcc^{BAT}$  whereas the right the  $SOAcc^{FT}$ . The blue dots in each case correspond to the values of  $SOAcc$  sampled every 1 h and the red dots the values of  $SOAcc$  sampled every 24 h. (For interpretation of the references to colour in this figure legend, the reader is referred to the web version of this article.)

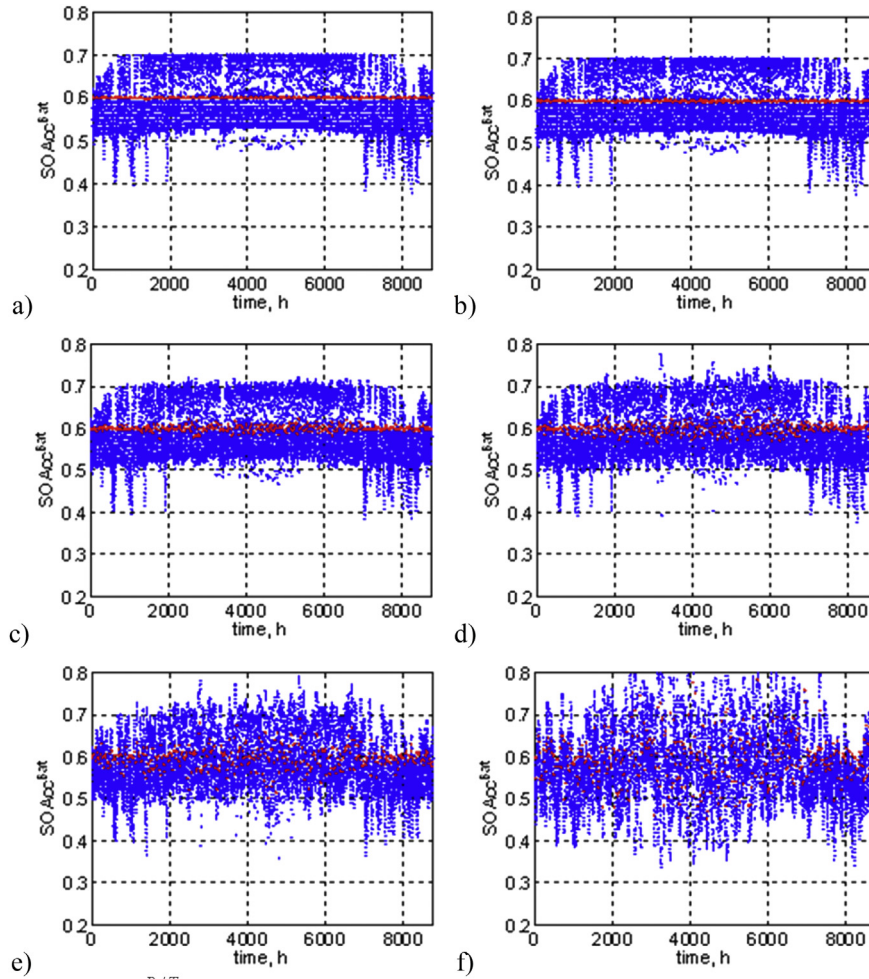


Fig. 12.  $SOAcc^{BAT}$  response when the variance is a) 0, b) 0.01, c) 0.05, d) 0.1, e) 0.2 and f) 0.5.

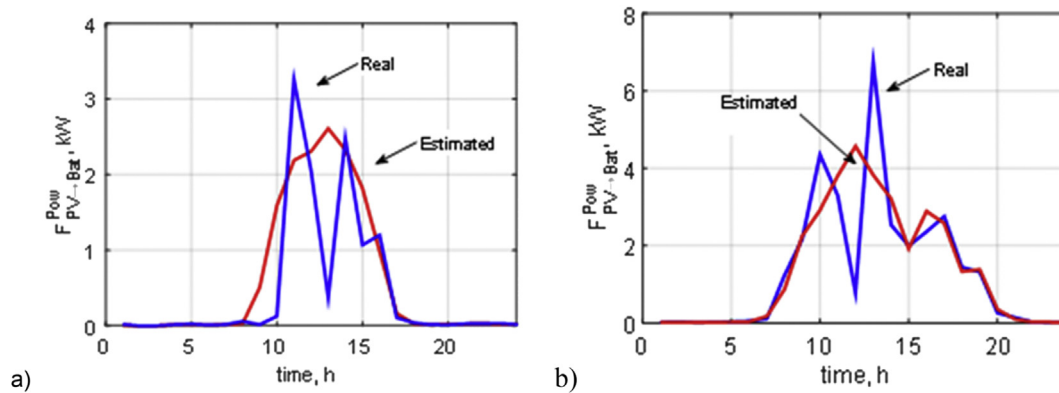


Fig. 13. The power produced from the PV during a) winter and b) summer. The blue trace is the real power produced (based on the actual weather emulated through the probability distribution approach) and the red trace is the assumed (estimated) one when the response of the  $SOAcc^{BAT}$  was based on the weather forecast using the original historical data. (For interpretation of the references to colour in this figure legend, the reader is referred to the web version of this article.)

### 5.2.2. Non-ideal weather forecasting

In this section we further investigate the aforementioned methodology by introducing an error in the estimation of the weather forecast and by assuming that the maximum power that we can operate the EL is at 30 kW. The error was imposed on the available yearly historical data by multiplying each sample of the power produced by the PV with a random number obtained from

a normal distribution with mean 1 and variable variance. As a case study this variance takes the values of 0, 0.01, 0.05, 0.1, 0.2 and 0.5 hence the distribution used for the error in the weather predictions changes at every time sample emulating different potential weather conditions. The yearlong response for these cases is shown in Fig. 12, and we can see that when the real and the predicted weather profiles are not the same, there is a

deviation between the real and the estimated PGCC and obviously for high values of this variance the 3 conditions are barely met. Having said that, we need to stress the fact that when the variance gets a value greater than 0.1, the distortion in the power delivered by the *PV* is significant and probably unrealistic. Fig. 13 shows the real and predicted power delivered by the *PV* to the *BAT* when the variance is 0.5 for two particular days and we can clearly see this difference which is unrealistic when a proper weather forecast is used for the next 24 h. It is therefore worth noting that the proposed method maintains the system within operating limits for reasonable weather forecasting errors. For more intense variability, the proposed method may still have beneficial results in its current form by actions such as considering smaller prediction and control intervals where forecasts may be better.

## 6. Conclusions

This work has presented a new approach which exploits the concept of PGCC to develop efficient PMS in the course of operation of a hybrid microgrid including energy storage. The proposed approach breaks down the operation of the system into several steps within a short time interval depending on the desired operating limits. The PGCC that indicates the temporal profile of the stored energy is shifted independently within each step in order to identify the amount of energy that needs to be utilized (produced or consumed) internally by the system and avoid the violation of important operating goals. Such operating goals include the avoidance of using outsourced energy supply, of overcharging particular accumulators, of wasting renewable energy at instants of high availability and of allowing incomplete charge-discharge cycles of accumulators which may have detrimental effects on the anticipated life term. Different parts of the shifted PGCC indicate different energy recovery or utilization targets which are matched by a sequence of control actions that activate desired converters for the appropriate duration in order to meet the desired operating goals.

The results obtained from the case studies indicate major advantages of identifying and implementing the most efficient PMS in the course of the system operation than selecting a PMS from a set of pre-specified ones as in Ref. [6]. The operating limits are never violated and the system always satisfies the operating goals. In this respect the use of outsourced electricity is completely avoided (i.e. the *DSL* is never activated), no renewable energy is wasted (i.e. the *PV* are not deactivated), the *BAT* is never overcharged while it always completes a full charge-discharge cycle from start to end of an operating time interval. Furthermore, the proposed approach facilitates the protection of delicate equipment such as the *FC* and the *EL* as they are activated very infrequently and with a short duration. Note that costs or profits may be linked to the operation of the system by considering the operating limits *Lo*, *Up*, *End*. Compared to cases where such limits are violated, avoiding in this work their violation means that the method may be used to minimize or maximize costs or profits. This is because expenditures are not needed for outsourced electricity supply, profits can be made from selling the renewable energy to the grid, the fact that we have full control of the energy inventories means that it is possible to achieve complete charge-discharge cycles which are also propagated to the converters and support a more controlled operation. This helps to establish a repetitive schedule of operation for the conversion and storage equipment, which generally reduces the wear and tear and enables less frequent maintenance. In this context, the very important and practical goals represented by the considered operating limits can be linked to cost or profit functions. On the other hand, it is beyond the scope of this work to investigate whether the considered limits can support a complete and exhaustive account of the terms required in cost and profit functions to fully characterize the economic performance of such a system.

## Appendix

**Table A.1**  
Generic model of power management strategy structure.

Connection	Symbol	Equation
<i>PV</i> → <i>BAT</i>	$\epsilon_{PV}(t)$	$\cap[\epsilon_{PV}^c(t)], c \in \{Avl, Req, Gen\}$
	$\epsilon_{PV}^{Avl}(t)$	1
	$\epsilon_{PV}^{Req}(t)$	$\rho_{PV}^{SOAcc^{BAT}}(t)$
	$\epsilon_{PV}^{Gen}(t)$	1
	$\rho_{PV}^{SOAcc^{BAT}}(t)$	$SOAcc^{BAT}(t) < Up_{PV}^{SOAcc^{BAT}}(t)$
	$\epsilon_{DSL}(t)$	$\cap[\epsilon_{DSL}^c(t)], c \in \{Avl, Req, Gen\}$
<i>DSL</i> → <i>BAT</i>	$\epsilon_{DSL}^{Avl}(t)$	1
	$\epsilon_{DSL}^{Req}(t)$	$\rho_{DSL}^{SOAcc^{BAT}}(t)$
	$\epsilon_{DSL}^{Gen}(t)$	1
	$\rho_{DSL}^{SOAcc^{BAT}}(t)$	$[SOAcc^{BAT}(t) < Up_{DSL}^{SOAcc^{BAT}}(t)] \vee$ $[Lo_{DSL}^{SOAcc^{BAT}}(t) < SOAcc^{BAT}(t) < Up_{DSL}^{SOAcc^{BAT}}(t)] \wedge$ $[ \epsilon_{DSL}^c(t-1) ]$
	$\epsilon_{CP}(t)$	$\cap[\epsilon_{CP}^c(t)], c \in \{Avl, Req, Gen\}$
	<i>CP</i> → <i>FT</i>	$\epsilon_{CP}^{Avl}(t)$
$\epsilon_{CP}^{Req}(t)$		$\rho_{CP}^{SOAcc^{FT}}(t)$
$\epsilon_{CP}^{Gen}(t)$		1
$\rho_{CP}^{SOAcc^{BF}}(t)$		$[SOAcc^{BF}(t) > Lo_{CP \rightarrow FT}^{SOAcc^{BF}}(t)] \vee$ $[Lo_{CP}^{SOAcc^{BF}}(t) < SOAcc^{BF}(t) < Up_{CP}^{SOAcc^{BF}}(t)] \wedge$ $[ \epsilon_{CP \rightarrow FT}^c(t-1) ]$
$\rho_{CP}^{SOAcc^{FT}}(t)$		$SOAcc^{FT}(t) < Up_{CP}^{SOAcc^{FT}}(t)$

(continued on next page)

Table A.1 (continued)

Connection	Symbol	Equation
$FC \rightarrow BAT$	$e_{FC}(t)$	$\rho_{FC}^c(t)$ , $c \in \{Avl, Req, Gen\}$
	$e_{FC}^{Avl}(t)$	$\rho_{FC}^{SOAcc^c}(t)$ , $l \in \{FT, WT\}$
	$e_{FC}^{Gen}(t)$	1
	$e_{FC}^{Req}(t)$	$\rho_{FC}^{SOAcc^{BAT}}(t)$
	$\rho_{FC}^{SOAcc^{FT}}(t)$	$SOAcc^{FT}(t) > Lo_{FC}^{SOAcc^{FT}}$
	$\rho_{FC}^{SOAcc^{WT}}(t)$	$SOAcc^{WT}(t) < Up_{FC}^{SOAcc^{WT}}(t)$
	$\rho_{FC}^{SOAcc^{BAT}}(t)$	$\int 1, [t = t_0] \vee [t = T - 1 \wedge \Delta S < 0]$ $\int 0, \text{ Otherwise}$
$EL \rightarrow BF$	$e_{EL}(t)$	$\rho_{EL}^c(t)$ , $c \in \{Avl, Req, Gen\}$
	$e_{EL}^{Req}(t)$	$\rho_{EL}^{SOAcc^{BF}}(t)$
	$e_{EL}^{Avl}(t)$	$\rho_{EL}^{SOAcc^c}(t)$ , $l \in \{BAT, WT\}$
	$e_{EL}^{Gen}(t)$	1
	$\rho_{EL}^{SOAcc^{BF}}(t)$	$SOAcc^{BF}(t) < Up_{EL}^{SOAcc^{BF}}(t)$
	$\rho_{EL}^{SOAcc^{BAT}}(t)$	$\int 1, [t = t_{up} - 1] \vee [t = T - 1 \wedge \Delta S > 0]$ $\int 0, \text{ Otherwise}$
	$\rho_{EL}^{SOAcc^{WT}}(t)$	$SOAcc^{WT}(t) > Lo_{EL}^{SOAcc^{WT}}(t)$

## References

- [1] S. Bandyopadhyay, Design and optimization of isolated energy systems through pinch analysis, *Asia-Pac J. Chem. Eng.* 6 (2011) 518–526.
- [2] N. Bizon, M. Oproescu, M. Raceanu, Efficient energy control strategies for a standalone renewable/fuel cell hybrid power source, *Energ Convers. Manag.* 90 (2015) 93–110.
- [3] M. Castañeda, A. Cano, F. Jurado, H. Sánchez, L.M. Fernández, Sizing optimization, dynamic modeling and energy management strategies of a stand-alone PV/hydrogen/battery-based hybrid system, *Int. J. Hydrogen Energy* 38 (10) (2013) 3830–3845.
- [4] A. Chauhan, R.P. Saini, A review on Integrated Renewable Energy System based power generation for stand-alone applications: configurations, storage options, sizing methodologies and control, *Renew. Sust. Energy Rev.* 38 (2014) 99–120.
- [5] I.J. Esfahani, S.C. Lee, C.K. Yoo, Extended-power pinch analysis (EPoPA) for integration of renewable energy systems with battery/hydrogen storages, *Renew. Energy* 80 (2015) 1–14.
- [6] D. Giaouris, A.I. Papadopoulos, S. Voutetakis, S. Papadopoulou, S. Seferlis, A power grand composite curves approach for analysis and adaptive operation of renewable energy Smart Grids, *Clean Technol. Environ. Policy* 17 (5) (2015) 1171–1193.
- [7] D. Giaouris, A.I. Papadopoulos, C. Ziogou, D. Ipsakis, S. Voutetakis, S. Papadopoulou, P. Seferlis, F. Stergiopoulos, C. Elmasides, Performance investigation of a hybrid renewable power generation and storage system using systemic power management models, *Energy* 61 (2013) 621–635.
- [8] W.S. Ho, H. Hashim, J.S. Lim, J.J. Klemes, Combined design and load shifting for distributed energy system, *Clean Technol. Environ. Policy* 15 (2013) 433–444.
- [9] W.S. Ho, C.S. Khor, H. Hashim, S. Macchietto, J.J. Klemes, SAHPPA: a novel power pinch analysis approach for the design of off-grid hybrid energy systems, *Clean Technol. Environ. Policy* 16 (5) (2013) 957–970.
- [10] W.S. Ho, Z.W.M.T. Mohd, H. Haslenda, A.M. Zarina, Electric system cascade analysis (ESCA): solar PV system, *Int. J. Electr. Power* 54 (2014) 481–486.
- [11] D. Ipsakis, S. Voutetakis, P. Seferlis, F. Stergiopoulos, S. Papadopoulou, C. Elmasides, The effect of the hysteresis band on power management strategies in a stand-alone power system energy, *Energy* 33 (2008) 1537–1550.
- [12] D. Ipsakis, S. Voutetakis, P. Seferlis, F. Stergiopoulos, C. Elmasides, Power management strategies for a stand-alone power system using renewable energy sources and hydrogen storage, *Int. J. Hydrogen Energy* 34 (16) (2009) 7081–7095.
- [13] C. Ziogou, D. Ipsakis, C. Elmasides, F. Stergiopoulos, S. Papadopoulou, P. Seferlis, S. Voutetakis, Automation infrastructure and operation control strategy in a stand-alone power system based on renewable energy sources, *J. Power Sources* 196 (22) (2011) 9488–9499.
- [14] J.J. Klemes (Ed.), *Process Integration Handbook*, Woodhead Publishing, Cambridge, UK, 2013.
- [15] J.J. Klemes, P.S. Varbanov, Process intensification and integration: an assessment, *Clean Technol. Environ. Policy* 15 (2013) 417–422.
- [16] Y.A. Kuznetsov, *Elements of Applied Bifurcation Theory*, Springer-Verlag, Berlin, Germany, 2004.
- [17] B. Linhoff, J.R. Flower, Synthesis of heat exchanger networks: I. Systematic generation of energy optimal networks, *AIChE J.* 24 (4) (1978) 633–642.
- [18] N.E. Mohammad Rozali, S.R. Wan Alwi, J.J. Klemes, M. Yusri Hassan, A process integration approach for design of hybrid power systems with energy storage, *Clean Technol. Environ. Policy* 17 (7) (2015) 2055–2072.
- [19] N.E. Mohammad Rozali, S.R. Wan Alwi, Z.A. Manan, J.J. Klemes, M.Y. Hassan, Cost-effective load shifting for hybrid power systems using power pinch analysis, *Energy Procedia* 61 (2014) 2464–2468.
- [20] N.E. Mohammad Rozali, S.R. Wan Alwi, Z.A. Manan, J.J. Klemes, M.Y. Hassan, Process integration techniques for optimal design of hybrid power systems, *Appl. Therm. Eng.* 61 (2013) 26–35.
- [21] N.E. Mohammad Rozali, S.R. Wan Alwi, Z.A. Manan, J.J. Klemes, M.Y. Hassan, Process integration of hybrid power systems with energy losses considerations, *Energy* 55 (2013) 38–45.
- [22] N.E. Mohammad Rozali, S.R. Wan Alwi, Z.A. Manan, J.J. Klemes, M.Y. Hassan, Optimisation of pumped-hydro storage system for hybrid power system using power pinch analysis, *Chem. Eng. Trans.* 35 (2013) 85–90.
- [23] N.E. Mohammad Rozali, S.R. Wan Alwi, Z.A. Manan, J.J. Klemes, M.Y. Hassan, Optimal sizing of hybrid power systems using power pinch analysis, *J. Clean. Prod.* 71 (2014) 158–167.
- [24] G.S.K. Priya, S. Bandyopadhyay, Emission constrained power system planning: a pinch analysis based study of Indian electricity sector, *Clean Technol. Environ. Policy* 15 (2013) 771–782.
- [25] R. Smith, *Chemical Process: Design and Integration*, John Wiley and Sons, New York, USA, 2005.
- [26] P.S. Varbanov, Z. Fodor, J.J. Klemes, Total site targeting with process specific minimum temperature difference ( $\Delta T_{min}$ ), *Energy* 44 (1) (2012) 20–28.
- [27] S.R. Wan Alwi, N.E.M. Rozali, Z.A. Manan, J.J. Klemes, A process integration targeting method for hybrid power systems, *Energy* 44 (2012) 6–10.
- [28] S.R. Wan Alwi, N.E.M. Rozali, Z.A. Manan, J.J. Klemes, Design of hybrid power systems with energy losses, *Chem. Eng. Trans.* 29 (2012) 121–126.
- [29] S.R. Wan Alwi, O.S. Tin, N.E.M. Rozali, Z.A. Manan, J.J. Klemes, New graphical tools for process changes via load shifting for hybrid power systems based on power pinch analysis, *Clean Technol. Environ. Policy* 15 (2013) 459–472.
- [30] H. Zahboune, F.Z. Kadda, S. Zouggar, E. Ziani, J.J. Klemes, P.S. Varbanov, Y. Zarhloule, The new electricity system cascade analysis method for optimal sizing of an autonomous hybrid PV/wind energy system with battery storage, in: 5th International Renewable Energy Congress (IREC) 2014, 2014, <http://dx.doi.org/10.1109/IREC.2014.6826962>.